

# Some studies on the axial injection system for a compact cyclotron

N. Hazewindus

*Philips Research Laboratories, Eindhoven, Netherlands*

## ABSTRACT

Two problems are discussed: the influence of space charge in the electrostatic lenses of the guiding system of an axial injection system and the design of a bunching system.

A calculation of the influence of a two-dimensional Gaussian space charge distribution on linear beam optics is presented. It is shown that quadrupole settings calculated using the space charge distribution agree much better with the experimentally observed settings than those obtained from calculations neglecting space charge.

The use of a klystron-type buncher is considered in order to increase the current accepted by the cyclotron. The simple bunching theory, ignoring the finite extent of the incoming beam, is used to obtain preliminary values of modulation voltage and drift space length. It is shown that the modulation does not seriously affect the emittance of the axial injection system nor the acceptance of the cyclotron centre. A detailed quantitative description of debunching effects due to the finite beam size is presented. Debunching effects limit the predicted current increase to a factor of between 2 and 2.5.

## 1. INTRODUCTION

A description of the axial injection system for the Philips prototype compact cyclotron has been given recently.<sup>1, 2</sup> Present operational experience shows that the deuteron current which can be put through the beam guiding system towards the deflector (through a 1 cm diam. hole in the pole faces) is limited to about 1.4 mA at 7.5 kV. An increase in this current may be obtained either by improvement of the ion source (e.g. increasing the luminosity), or by improvement of the ion optics of the quadrupole lens system, taking the space charge into account. For this purpose we developed a method for calculating space charge influence on linear beam optics. This method and its application are discussed in Section 2.

A larger accelerated current can also be obtained by bunching the current

emerging from the axial injection system.<sup>3</sup> An analysis of bunching and debunching effects in axial injection systems, leading to a design of a suitable bunching system for the compact cyclotron, is described in Section 3.

## 2. SPACE CHARGE CALCULATIONS

### 2.1. Introduction

The ion-optical properties of the beam guiding system are seriously changed due to space charge effects at beam current densities of several mA/cm<sup>2</sup> and energies of the order of 10 keV as are used at present in our axial injection system.

We shall calculate particle orbits through the guiding system, represented in two phase planes. A space charge term is included which follows from a two-dimensional Gaussian space charge distribution. A similar method for homogeneous beams, given by Kapchinskij and Vladimirkij<sup>4</sup> has recently been used by Resmini *et al*<sup>5</sup> for calculations on the Berkeley injection system.

### 2.2. Method of calculations

We consider a beam of particles, moving in the  $z$ -direction, with an elliptical cross-section:

$$\left(\frac{x}{x_M}\right)^2 + \left(\frac{y}{y_M}\right)^2 = 1$$

The eccentricity  $\alpha$  of the ellipse is  $\alpha = y_M/x_M$ ,  $x_M$  and  $y_M$  being its semi-axes. We represent the beam by a number of points in the  $x, x'$  and  $y, y'$  phase planes. Only particle motion in the  $x, z$  and  $y, z$  planes is considered. The values of  $x_M$  and  $y_M$  are found as the  $x$  and  $y$ -co-ordinates of those points in the  $x, x'$  and  $y, y'$  planes which have the largest distance from the  $x'$  and  $y'$  axis respectively. We assume that the cross-section of the beam will remain elliptical when traversing the guiding system (see Section 2.4).

For the space charge density we take the following two-dimensional Gaussian distribution:

$$\rho(x, y) = c. \exp \left[ - \left( \frac{x}{x_B} \right)^2 - \left( \frac{y}{y_B} \right)^2 \right], x \leq x_M, y \leq y_M$$

where  $c$  is a constant to be determined later and  $x_B$  and  $y_B$  are related to the beam semi-axes by  $x_M/x_B = y_M/y_B = \gamma$ , a constant defining the 'flatness' of the distribution in the beam cross-section.

A point  $P$  with co-ordinates  $x_p$  and  $y_p$  lies on an ellipse with semi-axes  $x_0$  and  $y_0$ , where  $x_0/x_B = y_0/y_B = \beta$ . The space charge density in  $P$  is then:

$$\rho(x_p, y_p) = c. \exp (-\beta^2).$$

If the beam current is  $I$  and the particle velocity is  $v$ , the constant  $c$  can now be determined. One finds for the space charge distribution:

$$\rho(x, y) = \frac{I \exp(-\beta^2)}{\pi \alpha v x_B^2 [1 - \exp(-\gamma^2)]}$$

In order to find the field strength originating from this charge distribution we assume that the equi-potential lines  $V(x, y)$  have also an elliptical shape with eccentricity  $\alpha$  (see Section 2.4). Then the electric field strength in point  $P$  equals:

$$E(x_p, y_p) = \frac{E_0}{\sqrt{\left(\frac{x_p}{x_0}\right)^2 (1 - \alpha^2) + \alpha^2}}$$

Now  $E_0$  is found by applying Gauss's law. We obtain:

$$E_0 = \frac{I}{4x_0 v \epsilon_0 A} \cdot \frac{1 - \exp(-\beta^2)}{1 - \exp(-\gamma^2)}$$

with  $\epsilon_0$  the dielectric constant in vacuo. The factor  $A$  is found from:

$$A = \int_0^1 \frac{\xi^2(\alpha^2 - 1) + 1}{-\xi^4(1 - \alpha^2) + (1 - 2\alpha^2)\xi^2 + \alpha^2} d\xi$$

### 2.3. Numerical integration

The beam is represented by a number of points in the  $x, x'$  and  $y, y'$  planes, as stated above. From the values of the initial co-ordinates  $x_M$  and  $y_M$  are found. Hence  $\alpha$  is known and the integral  $A$  can be numerically calculated. If the point  $P$  lies in the  $x$ - $z$  plane, the field strength  $E$  is:

$$E = \frac{I}{4x_p v \epsilon_0 A} \cdot \frac{1 - \exp\left[-\gamma^2 \left(\frac{x_p}{x_M}\right)^2\right]}{1 - \exp(-\gamma^2)}$$

and if it lies in the  $y$ - $z$  plane, we get:

$$E = \frac{I}{4y_p v \epsilon_0 A} \cdot \frac{1 - \exp\left[-\gamma^2 \left(\frac{y_p}{\alpha x_M}\right)^2\right]}{1 - \exp(-\gamma^2)}$$

For all points considered, the equations of motion are integrated along a short interval  $dz$ . Inspection of the positions of the points in the phase planes leads to a new value for  $\alpha$  (as shown in Section 2.2). Then the integration is repeated, using the same value of  $\gamma$ .

In the computer programme, written in ALGOL-60, beam passage through drift lengths and quadrupole lenses is covered. A second programme, based on the same principle of space charge calculation, has been made to compute orbits in the cyclotron central region.<sup>6</sup>

#### 2.4. Discussion

Two assumptions made earlier, namely (1) the beam cross-section remains elliptic, and (2) the lines of constant  $V$  are ellipses with the same  $\alpha$  as the lines of constant  $\rho$ , need some further discussion.

Consider particles moving in a plane  $x_1, z_1$  parallel to the  $x, z$  plane. Here the width of the beam is smaller by a factor of  $d$ . The points representing the beam in the corresponding  $x_1, x_1'$  phase plane must occupy a surface of the same shape as those in the  $x, x'$  plane. A similar requirement for the  $y, y'$  phase spaces is needed. The beam cross-section then remains elliptical on passing through drift spaces and quadrupole lenses, but it can be shown that space charge forces will cause deviations from this shape when  $\alpha$  differs from unity.

The equipotential lines have the same  $\alpha$  as the lines of constant  $\rho$  only if  $\alpha = 1$  (circle) as can be readily demonstrated by applying Poisson's law to the chosen forms of  $V$  and  $\rho$ .

Though the present representation is not strictly correct it seems to us that it is a quite reasonable approximation for those cases in which beams with an  $\alpha$  not deviating too much from unity are calculated and for which the influence of space charge may still be considered as a correction to the ion-optical properties.

#### 2.5. Results

The influence of space charge on a symmetric, 1600 mm mrad, 7.5 kV deuteron beam passing through a 25 cm long drift space is shown in Figs 1 and 2. The broadening of the beam when current is increased from zero to 3 mA is shown in curves *a* and *b*. The motion remains linear when the charge distribution is homogeneous (curve *b*,  $\gamma = 0.01$ ), but when charge is initially concentrated in the central part of the beam (curves *c* and *d*,  $\gamma = 1$  and  $\gamma = 2$  respectively) the trajectories tend to move to the edges and the motion becomes non-linear.

In the next four figures we show the passage of a 500 mm mrad, 7.5 kV deuteron beam through an electrostatic quadrupole triplet (lens length 50 mm, internal diam. 30 mm), followed by a 17 cm long drift space. The shape of the initial phase space areas is estimated from the source geometry used. At the end of the last drift space a quadrupole lens doublet is situated.

In Figs 3 and 4 we show results belonging to values of the lens strength ( $K_1 = 18, K_2 = -20, K_3 = 16 \text{ m}^{-1}$ ) initially chosen from a series of calculations neglecting space charge. At the current level used (between 3 and 5 mA) especially the  $x$ -dimension of the beam gets too large. In Figs 5 and 6 we show results for enhanced quadrupole focusing ( $K_1 = 20, K_2 = -24, K_3 = 18 \text{ m}^{-1}$ ), values quite near to the ones experimentally observed ( $K_1 = 21, K_2 = -24, K_3 = 17 \text{ m}^{-1}$ ). Here, the size in the  $x$ -direction diminishes when the current increases, whereas that in the  $y$ -direction slowly increases.

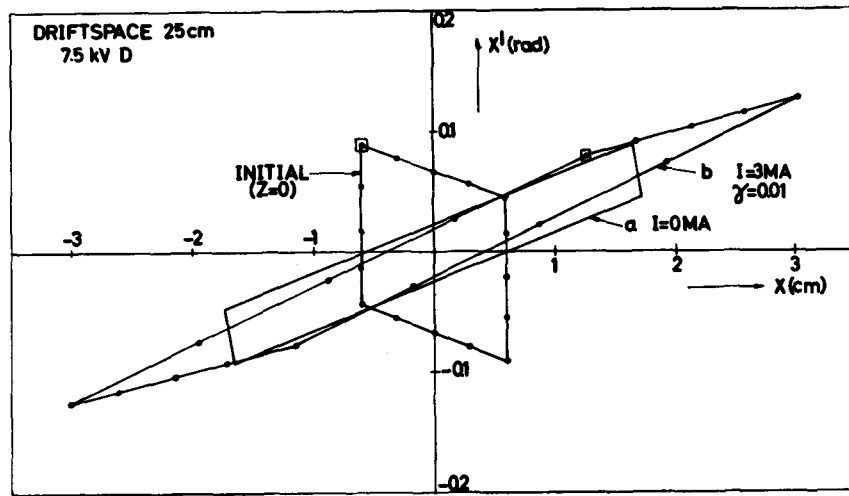


Fig. 1. Influence of a homogeneous current distribution on a symmetric 1600 mm mrad, 7.5 kV deuteron beam, passing through a 25 cm drift space

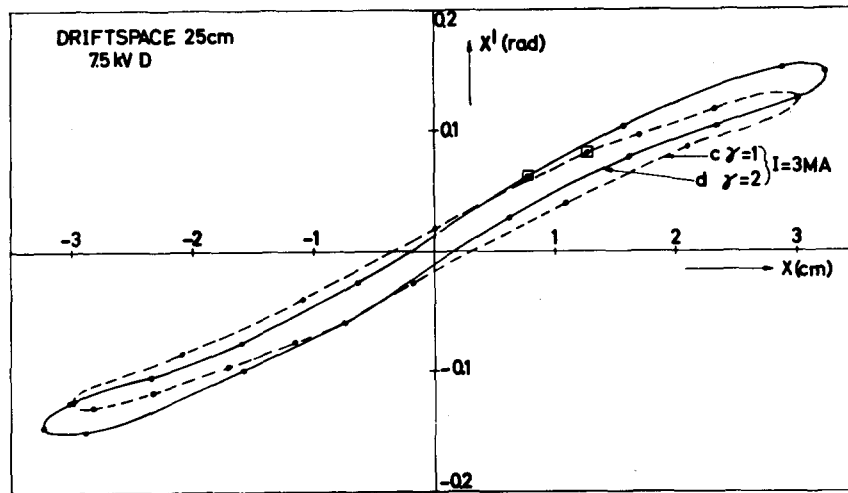


Fig. 2. Same as Fig. 1, but with a Gaussian current distribution

From these and other figures it seems that the current will be limited to about 3 mA, as otherwise the beam size in the  $x$ -dimension will be too large. The conclusion is supported by an observed current of 2.8 mA on a target at 2.5 cm behind this quadrupole system, when focusing is adjusted to optimum transmission. The current on this target can be enlarged by choosing other quadrupole settings, but then it is experimentally observed that the current transmitted through the total system drops.

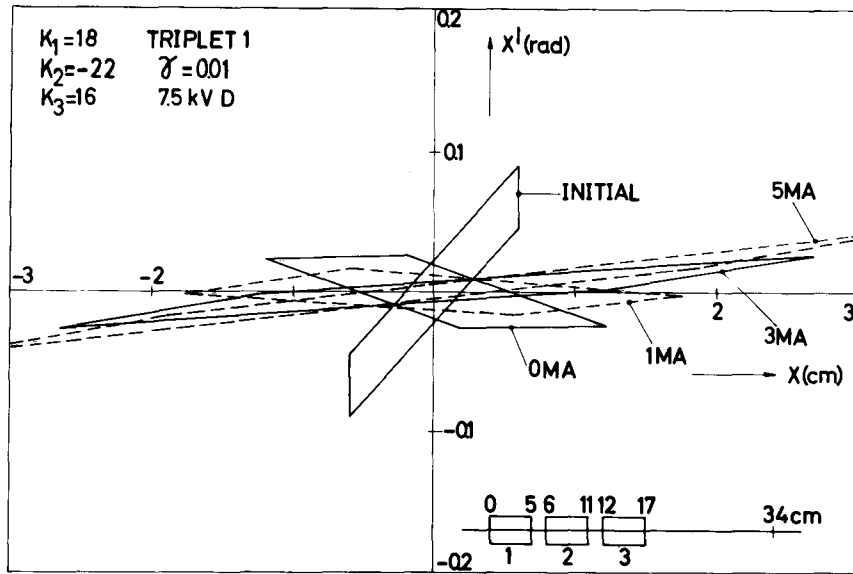


Fig. 3. Horizontal phase planes between the first quadrupole triplet. Settings from calculations neglecting space charge

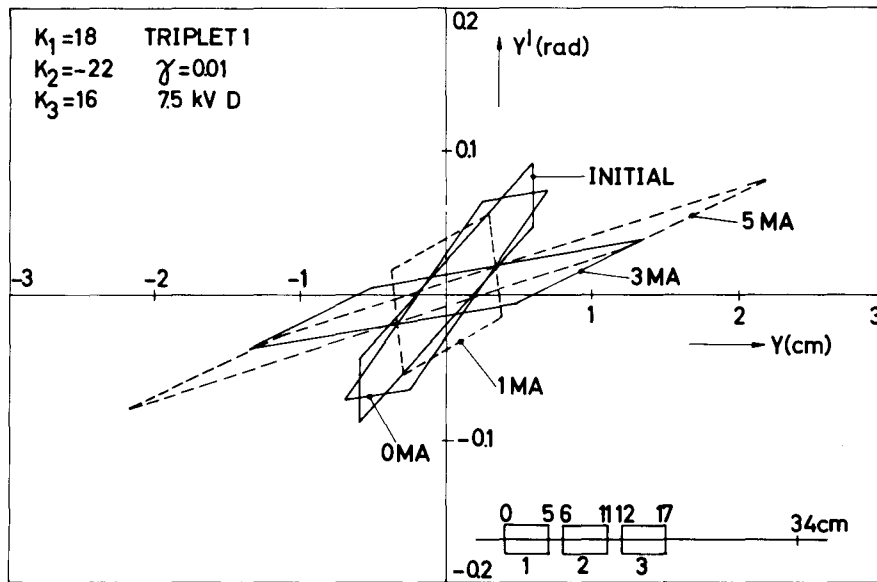


Fig. 4. As Fig. 3, vertical phase planes

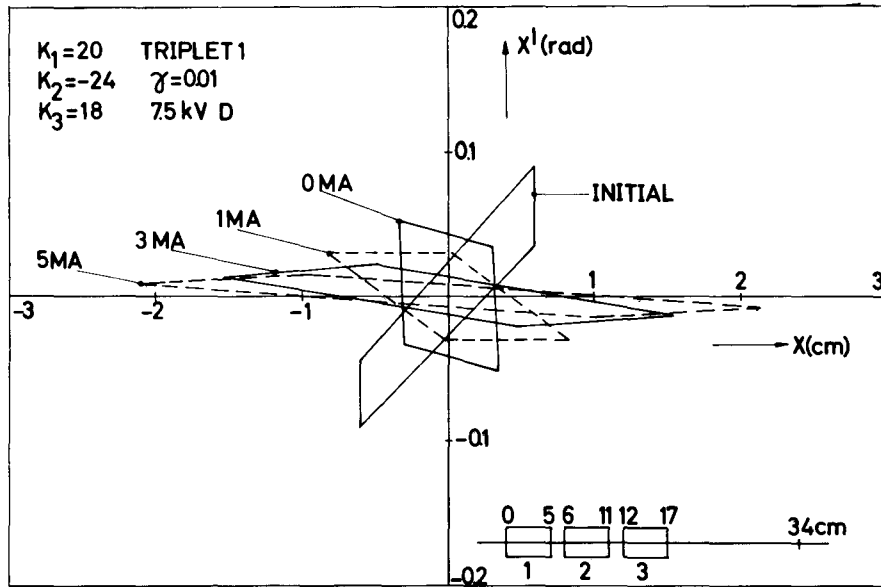


Fig. 5. As Fig. 3, increased focusing optimised for  $i = 3$  mA

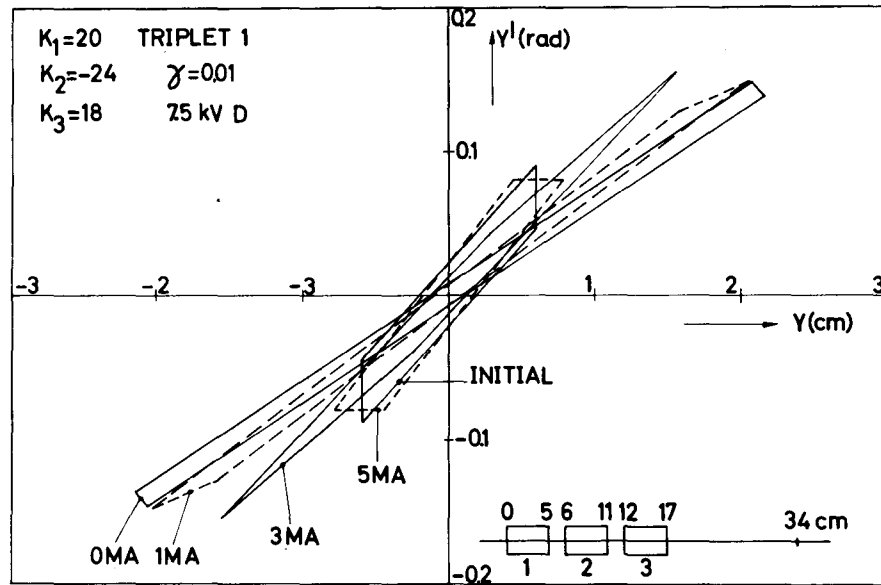


Fig. 6. As Fig. 4, increased focusing optimised for  $i = 3$  mA

A calculation of all quadrupole settings is at present being performed. The first results indicate that at 7.5 keV deuteron energy 3 mA must be considered as an upper limit in the present system.

### 3. CALCULATIONS ON A BUNCHING SYSTEM

#### 3.1. Introduction

In a klystron-type<sup>7</sup> buncher a small sinusoidal modulating voltage  $V_m \sin n\omega t$  (with  $\omega$  the particle angular velocity in the cyclotron and  $n$  the harmonic number of the accelerating rf field) is applied to a beam of particles with energy  $eV_0$ . Bunches are formed in a drift space with length  $l$ .

The relation between the rf starting phase  $\varphi_0$  of a particle and its phase  $\varphi_1$  after traversing the drift space is:<sup>7</sup>

$$\varphi_1 = \varphi_t + \varphi_0 - \rho \sin \varphi_0$$

where  $\varphi_t = n\omega l/v_0$  (with  $v_0$  the initial particle velocity) is a constant for all particles and can hence be ignored. The factor  $\rho$ , the bunching parameter, is given by  $\rho = (n\omega l/2v_0) (V_m/V_0)$ . It must lie between 1.4 and 1.8 to obtain optimum bunching conditions.<sup>7</sup> We shall use this expression to choose, for a reasonable value of  $\rho$ , the initial values of  $V_m/V_0$  and  $l$ .

Due to the velocity modulation applied, the emittance of the axial injection system will vary in shape and position. Furthermore, the acceptance of the cyclotron centre can change for particles with different longitudinal velocities. We shall investigate whether these effects influence the matching of the axial injection system and the cyclotron central region.

After these considerations the debunching effects will be studied. Debunching is caused by:

- (a) energy spread of source and extractor,
- (b) different path lengths due to non-zero beam quality,
- (c) longitudinal space charge (especially for very short bunches).

In the following discussion the last named effect is not further treated.

#### 3.2. Matching of emittance and acceptance

An energy variation of  $\pm 0.5\%$  in the incoming beam is expected. We want a much higher value of the modulation depth and will use  $V_m/V_0 = 0.1$ . For  $\rho = \pi/2$  we then find  $l = 8$  cm when  $n = 4$ .

In a recent paper<sup>2</sup> we showed that the emittance of the axial injection system and the acceptance of the cyclotron centre are matched in a plane just behind the deflector. We now calculated the displacement of the emittance using our analytical formulas.<sup>8</sup> In the horizontal phase plane the shifts amount to  $\pm 0.1$  mm and  $\pm 0.025$  radians, and in the vertical phase plane  $\pm 0.5$  mm and 0 radians. These displacements will enlarge the emittance by about 20%.

The acceptance of the cyclotron centre was tested by calculating orbits starting with  $e(V_0 \pm 0.1 V_0)$  at several representative starting points.<sup>2</sup> The horizontal motion is hardly affected by this modulation: the orbit centre positions vary by less than 1.5 mm as is shown in Fig. 7 for a typical case. The vertical focusing does not change much either (see Fig. 8, same case as Fig. 7).

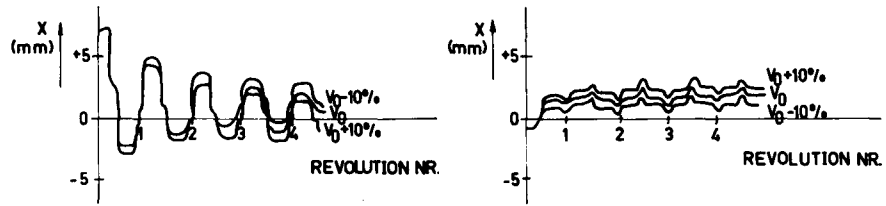


Fig. 7. Orbit centre displacements in x and y-direction for 10% modulation in starting energy

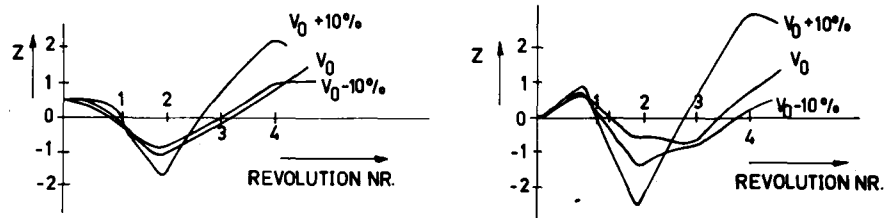


Fig. 8. Some vertical orbits for 10% modulation in starting energy

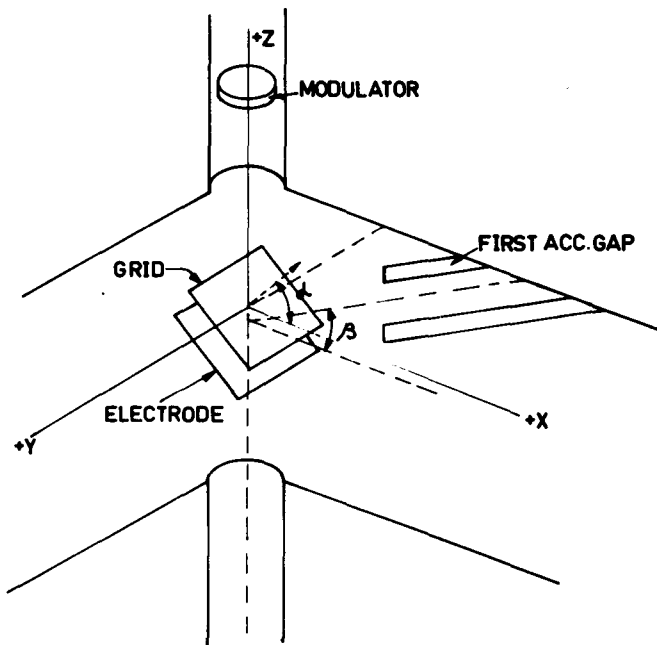


Fig. 9. The co-ordinate system used in the calculation

From these calculations we find that there will be only minor changes in the matching conditions between injection system and central region.

### 3.3. Definition of a co-ordinate system

Recently we derived analytical formulas representing particle motion through an axial injection system with a plane electrostatic deflector.<sup>8</sup> In the next section they are used to obtain detailed expressions. Here we shall briefly review the nomenclature used; a complete description is given in reference 8.

The calculations are performed in the  $x, y, z$  co-ordinate system shown in Fig. 9. The  $y$ -axis lies in the front plane of the deflector, whereas particles enter along the  $z$ -axis. Dimensionless momentum and co-ordinate values are used throughout the calculation. Momenta are made dimensionless by dividing by  $p_{z0}$ , the initial momentum of a particle with zero modulation travelling along the central orbit. Co-ordinates are divided by  $r$ , the radius of this particle in the cyclotron magnetic field. Thus:

$$X = \frac{x}{r}, \quad P_x = \frac{P_x}{p_{z0}}, \quad Y = \frac{y}{r}, \quad P_y = \frac{P_y}{p_{z0}}, \quad Z = \frac{z}{r}, \quad P_z = \frac{P_z}{p_{z0}}.$$

It is convenient to use time units  $\tau = \omega t$ .

The normal to the deflector is at an angle  $\alpha$  to the positive  $x$ -axis. The first accelerating gap, which is intersected at right angles by the central orbit, is at an angle  $\beta$  to the positive  $x$ -axis.

Values of momenta and co-ordinates at different places are denoted by subscripts  $i$  (e.g.  $X_i, P_{xi}$ , etc.) in the following manner:  $i = 0$  starting plane (situated in the field-free region),  $i = 1$  entrance of fringing field,  $i = 2$  exit of fringing field,  $i = 3$  entrance of deflector,  $i = 4$  exit of deflector,  $i = 5$  first accelerating gap.

The following transit times have been calculated for a particle travelling along the central orbit:

$\tau_f$  between starting point and fringing field (0-1)

$\tau_d$  between fringing field and deflector (2-3)

$\tau_m$  in the deflector (3-4)

$\tau_g$  between deflector and first accelerating gap.

After deflection, the horizontal orbit is characterised by its orbit centre co-ordinates  $X_c$  and  $Y_c$ , together with the radius  $R$ .

### 3.4. Formulas

For a particle travelling along an arbitrary paraxial path the differences in transit times  $\Delta\tau_f, \Delta\tau_d$ , etc., due to variations in the initial co-ordinates and momenta, can be calculated. We find:

$$\Delta\tau_f = \tau_f (1 + P_{z0})$$

$$\Delta\tau_d = X_2 + \sin \tau_d \cdot P_{x2} + (1 - \cos \tau_d) P_{y2} + \tau_d (P_{z2} + 1)$$

$$\Delta\tau_m = -\tau_m P_{x3} - \frac{1}{2} \tau_m^2 P_{y3} - \tau_m (1 + P_{z3})$$

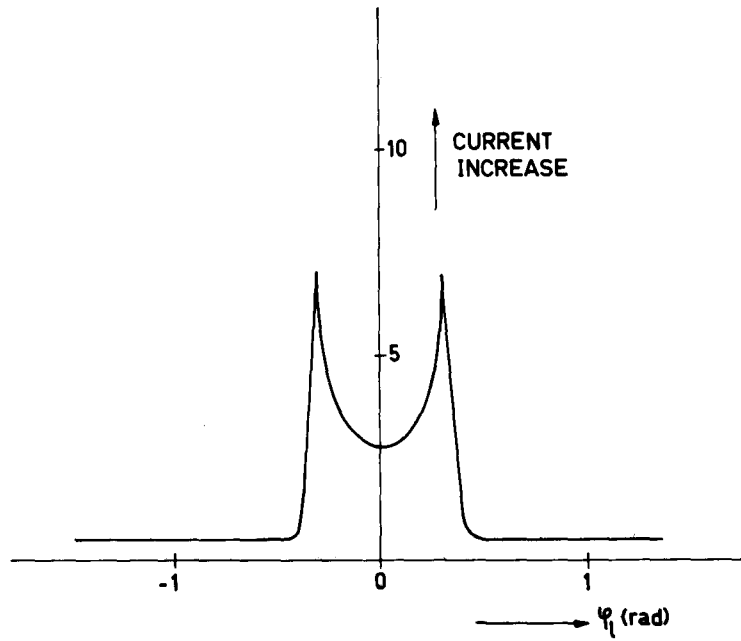


Fig. 10. Bunch shape neglecting debunching effects  
 ( $\rho = \pi/2$ ,  $V_m/V_0 = 0.1$ ,  $\tau_f = 4.97$ ,  $\tau_m = 1.88$ ,  $\beta = \pi/2$ )

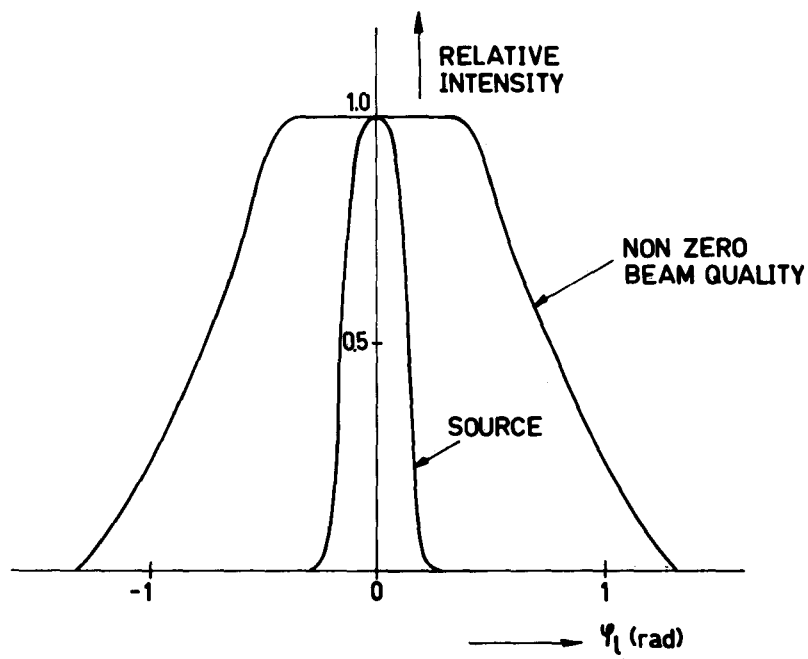


Fig. 11. Spread in arrival phase  $\phi_1$  due to non-zero beam quality and due to energy variations in the ion source

$$\Delta\tau_g = (1 - \cos \beta) X_c + \sin \beta \left( Y_c + \frac{1}{\tan \alpha} \right) + \left( \frac{1 - \cos \tau_m}{\tau_m \tan \alpha} - X_4 \right)$$

The total difference in transit time

$$\Delta\tau = \Delta\tau_f + \Delta\tau_d + \Delta\tau_m + \Delta\tau_g$$

can be expressed in the initial co-ordinates and momenta as:

$$\Delta\tau = a_1 X_0 + a_2 P_{x0} + a_3 Y_0 + a_4 P_{y0} + a_5 (1 + P_{z0})$$

The coefficients  $a_1, a_2$ , etc., are found using transformations given in reference 8:

$$a_1 = \frac{1}{2} [1 - \cos \beta + (\tau_m - \sin \beta) (\sin \tau_d + \frac{1}{2} \tau_m \cos \tau_d)]$$

$$a_2 = -\sin \beta + \frac{1}{2} \tau_f (1 - \cos \beta) + (\tau_m - \sin \beta) \left[ \frac{1}{2} (\tau_f + \tau_m) \sin \tau_d + \frac{1}{4} \tau_f \tau_m - 1 \right] \cos \tau_d$$

$$a_3 = \frac{1}{2} [\sin \beta + (\tau_m - \sin \beta) (\frac{1}{2} \tau_m \sin \tau_d - \cos \tau_d)]$$

$$a_4 = \frac{1}{2} \tau_f \sin \beta + (1 - \cos \beta) + (\tau_m - \sin \beta) \left[ (\frac{1}{4} \tau_f \tau_m - 1) \sin \tau_d - \frac{1}{2} (\tau_f + \tau_m) \cos \tau_d \right]$$

$$a_5 = \tau_f + \tau_d + \sin \beta.$$

### 3.5. Calculations

For the compact cyclotron axial injection system the following parameters are given:  $\tau_d = 1.88$ ,  $\tau_m = 0.953$ , and  $\beta = \pi/2$ .

The place where the particles are modulated can now be determined accurately. A particle starting at  $\varphi_0 = \pi/2$  gets a velocity  $P_{z0} = 0.950$ . With the  $\rho$ -value used, the particle will have  $\varphi_l = 0$  at the end of the drift space. Thus, for  $\Delta\tau = \pi/8$  (since  $n = 4$ ) we obtain  $\tau_f = 4.97$ .

The shape of the bunch obtained in this case (neglecting all debunching effects) is shown in Fig. 10. The bunch width amounts to 0.75 radians.

We assume the incoming beam to occupy in both phase planes a rectangular surface of  $6 \times 84$  mm mrad. The spread in arrival phase  $\varphi_l$  due to non-zero beam quality was calculated by picking out at random a large number of particles from the incoming beam. For all these particles  $\varphi_0 = 0$  and  $P_{z0} + 1 = 0$ . The coefficients  $a_1, a_2, a_3$ , and  $a_4$  are found to be:  $a_1 = 0.481$ ,  $a_2 = 1.355$ ,  $a_3 = 0.482$ ,  $a_4 = 3.435$ . The distribution in arrival phase  $\varphi_l$  obtained is shown in Fig. 11, yielding a spread of 1.5 radians *FWHM*.

When the initial beam already has a 1% *FWHM* energy distribution, the resulting spread is shown also in Fig. 11. It amounts to 0.3 radians *FWHM*.

### 3.6. Conclusion

It is shown that the debunching originating from non-zero beam quality strongly determines the minimum bunch width that can be obtained from our system. The shape of the bunch can be found by superimposing the distribution due to

the debunching effects on the ideal bunch shape. Then we predict an improvement in current by a factor of between 2 and 2.5.

A better result might be obtained when the actual beam quality is better (e.g. if some of the beam were intercepted in the guiding system) or when the distribution of the particles over the co-ordinates and momenta is not homogeneous (as was assumed in the calculation of the debunching effects).

#### ACKNOWLEDGEMENTS

Discussions with Prof. Dr. H. L. Hagedoorn, Ir. R. A. Koolhof, Ir. J. M. van Nieuwland, and A. Petterson are gratefully acknowledged.

#### REFERENCES

1. Hazewindus, N., *I.E.E.E. Trans. Nucl. Sci.* **NS-16**, 459, (1969).
2. van Nieuwland, J. M. and Hazewindus, N., *I.E.E.E. Trans. Nucl. Sci.* **NS-16**, 454, (1969).
3. Powell, W. B., *I.E.E.E. Trans. Nucl. Sci.* **NS-13**, 147, (1966).
4. Kapchinskij, J. M. and Vladimirskij, V. V., International Conference on High-Energy Accelerators and Instrumentation, CERN 1959, 274.
5. Resmini, F. and Clark, D. J., *I.E.E.E. Trans. Nucl. Sci.* **NS-16**, 465, (1969).
6. Hagedoorn, H. L., Hazewindus, N., and van Nieuwland, J. M., Proceedings of this Conference, p. 274.
7. Hamilton, D. R. *et al*, Klystrons and microwave triodes, M.I.T. Rad. Lab. Series, 7, New York (1948).
8. Hazewindus, N., accepted for publication in *Nucl. Instr. Meth.*